ACS APPLIED MATERIALS & INTERFACES

Research Article

www.acsami.org

Thermal Conductive and Mechanical Properties of Polymeric Composites Based on Solution-Exfoliated Boron Nitride and Graphene Nanosheets: A Morphology-Promoted Synergistic Effect

Xieliang Cui,[†,‡] Peng Ding,[*,†] Nan Zhuang,[†] Liyi Shi,[*,‡] Na Song,[†] and Shengfu Tang[†]

[†]Research Center of Nanoscience and Nanotechnology, Shanghai University, 99 Shangda Road, Shanghai 200444, People's Republic of China

[‡]Department of Polymer Materials, Shanghai University, 99 Shangda Road, Shanghai 200444, People's Republic of China

Supporting Information

ABSTRACT: In this work, we reported a synergistic effect of boron nitride (BN) with graphene nanosheets on the enhancement of thermal conductive and mechanical properties of polymeric composites. Here, few layered BN (s-BN) and graphene (s-GH) were used and obtained by liquid exfoliation method. The polystyrene (PS) and polyamide 6 (PA) composites were obtained via solution blending method and subsequently hot-pressing. The experimental results suggested that the thermal conductivity (TC) of the PS and PA composites increases with additional introduction of s-BN. For example, compared with the composites containing 20 wt % s-GH, additional introduction of only 1.5 wt % s-BN could increase the TC up to 38 and 34% in polystyrene (PS) and polyamide 6 (PA) matrix, respectively. Meanwhile, the mechanical properties of the composites were synchronously enhanced. It was found that s-BN filled in the interspaces of s-GH sheets and formed s-BN/s-GH stacked structure, which were helpful for the synchronously improving TC and mechanical properties of the polymeric materials.

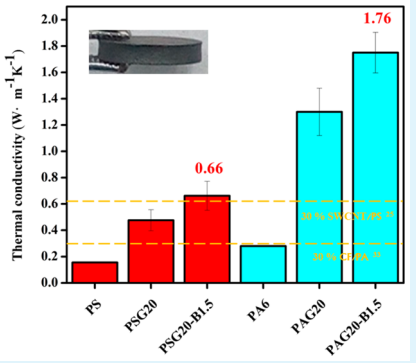

KEYWORDS: *thermal conductivity, graphene, boron nitride, solution-exfoliated, polymer*

1. INTRODUCTION

Thermal conductive polymeric composites have attracted considerable attention for their heat removal abilities in the fields of electronic devices, the semiconductor industry, and so on.[1] In this field, two-dimensional (2-D) materials such as graphene and boron nitride (BN), were proved to be a good choice as thermal conductive fillers for thermal transfer due to their superb thermal conductivity (TC), high surface area, and excellent mechanical properties.[2−4] Plenty of studies were mainly focus on obtaining the composites with high TC by these 2-D fillers and several strategies were generally carried out. For example, one steategy is to improve the affinity between fillers and polymer matrix, which strengthen the phonon coupling in the composites. TC of polyester matrix could be increased to 0.542 $W{\cdot}m^{-1}K^{-1}$ when introduced to covalently grafted graphene with only 1.45 vol % loading.[5] However, this approach associates with a functionalized/oxidized process of the fillers. Another strategy is using a very high filler loading, which is in favor of forming continuous thermal networks in the composites. For using 60 wt % graphite and carbon fiber (CF), the TC for polyamide (PA) increased from 0.2 to 2.03 $W{\cdot}m^{-1}K^{-1}$.[6] However, this approach was often limited by the loss of mechanical integrity of the polymer materials.[7]

Recently, several studies have been reported that suitable combinations of different fillers could obviously enhance the TC of the composites compared to individual filler at the same loadings. For example, Yu et al.[8] reported that the combined use of graphite nanoplatelets (GNPs, 7.5 wt %) and single-walled carbon nanotubes (SWCNTs, 2.5 wt %) could improve the TC from 0.2 to 1.75 $W{\cdot}m^{-1}K^{-1}$ for epoxy. The enhancement of TC surpassed the performance of the individual SWCNTs and GNPs fillers at 10 wt % filler loading. Yang et al.[9] reported that the combined use of multigraphene platelets (MGPs, 0.9 wt %) and multiwalled carbon nanotubes (MWCNTs, 0.1 wt %) in epoxy matrix achieved a maximum TC of 0.32 $W{\cdot}m^{-1}K^{-1}$, which was higher than the values obtained by performing individual MGPs and MWCNTs in the composites at 1 wt % loading. The above investigations proposed a mechanism that 1-D CNT linked the adjacent 2-D graphene sheets as a bridge and thus the extended area of the CNTs-graphene junctions was favor for the TC enhancement in the composites. Recently, Tsai et al.[10] obtained a TC ∼ 2.21 $W{\cdot}m^{-1}K^{-1}$ of polyimide film with 50 wt % functionalized BN and 1 wt % glycidyl-methacrylate-grafted graphene (g-TrG) hybrid filler. They explained that the voids between the BN filler and polymer matrix were filled by the graphene nanolayers and thus led to the high TC of the composites. Liem and Choy

Received: May 21, 2015
Accepted: August 17, 2015
Published: August 17, 2015

DOI: 10.1021/acsami.5b04444
ACS Appl. Mater. Interfaces 2015, 7, 19068−19075

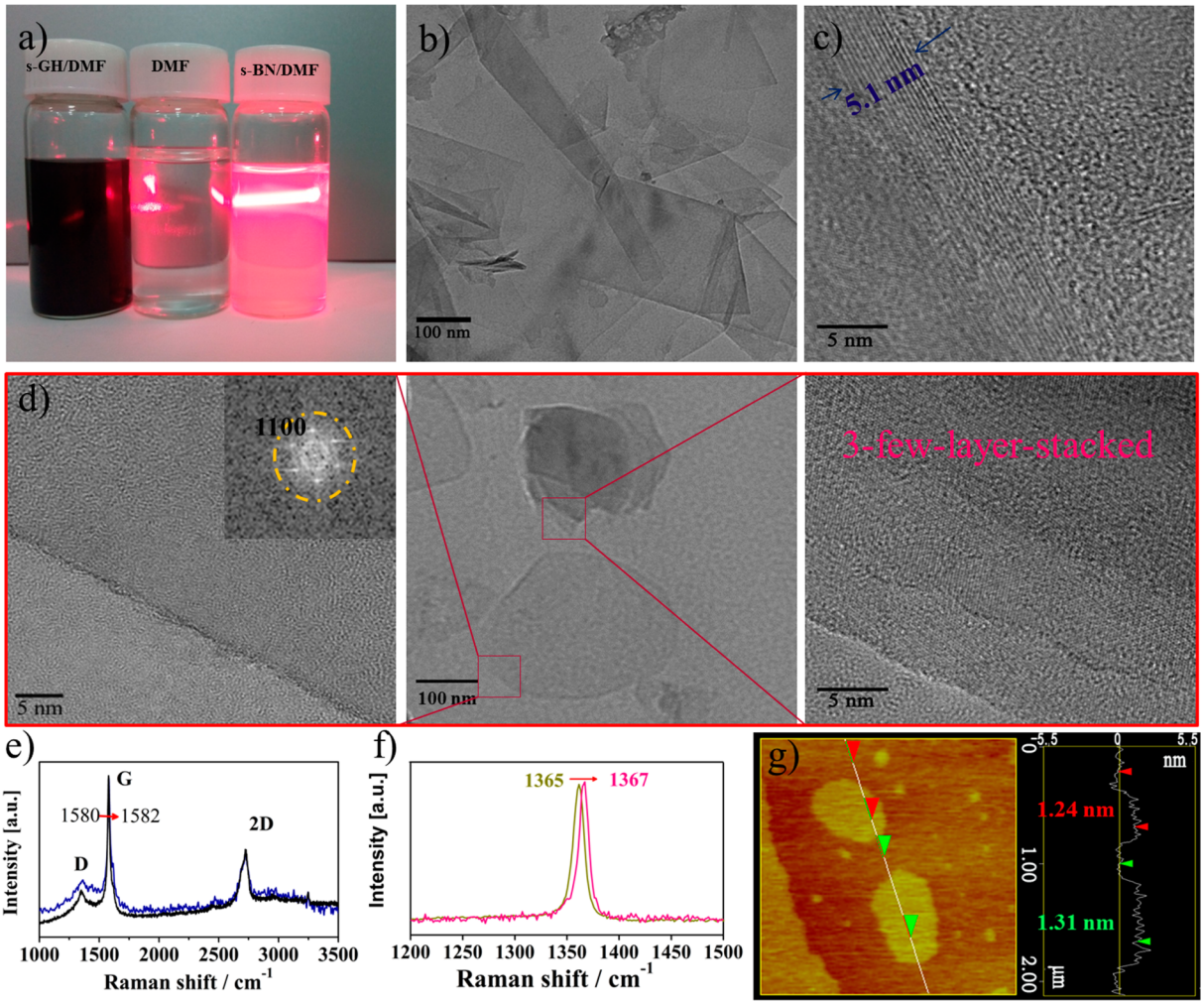

Figure 1. Exfoliation of GH and BN. (a) s-GH and s-BN sheets dispersed in DMF solutions for more than one month. (b) TEM image of s-GH. (c) HRTEM image of s-GH sheet. (d) TEM images of s-BN sheets, and its HRTEM images for selected areas and (inset) corresponding FFT of the image. (e) Raman spectra of GH at 514 nm excitation: (black) before and (blue) after sonication. (f) Raman spectra of BN: (dark yellow) before and (pink) after sonication. (g) AFM images of s-BN sheets.

also reported similar effects of pristine graphene with BN on the TC enhancement in epoxy matrix.[11]

In the present work, we reported a synergistic effect of BN with graphene on the enhancement of thermal conductive and mechanical properties of polymeric composites. Polystyrene (PS) was chosen as the matrix for the mechanism study of the synergistic effect without the interference of crystalline. Furthermore, we also observed the same enhance effect as this hybrid fillers applied for PA. Here, the widely used liquid exfoliation method was performed to obtain few layered BN (s-BN) and graphene (s-GH), which avoid the functionalized/oxidized process of the 2-D layers. Compared with the composites containing 20 wt % s-GH, additional introduction of only 1.5 wt % s-BN could increase the TC up to 38% and 34% in PS and PA matrix, respectively. Meanwhile, the mechanical properties of the composites were enhanced even with more than 20 wt % filler content. For example, the Young's modulus and microhardness of the PS composites increased from 4.3 to 6.3 GPa and from 0.14 to 0.25 GPa, respectively. A morphology-promoted synergistic effect was proposed based on the structure characterization, which showed that nanosized s-BN sheets filled into the s-GH interspaces and formed s-BN/s-GH stacked structure and thus resulted in the obvious enhancement of TC. As far as we know, the synergistic effect of small amount BN with graphene has not been observed previously in this way. The obtained polymeric materials could be applied in thermal interface materials, connectors, and other high-performance thermal management systems.

2. EXPERIMENTAL SECTION

2.1. Materials and Equipment. Graphene (GH) nanoplatelets (6−8 nm thick × 5 μm wide) were purchased from Strem Chemicals (Newburyport, MA). PS (Mw ∼ 192 000 g/mol, 1.076 g/cm^3), PA (pellets, 3 mm, 1.084 g/cm^3), h-BN power (1 μm) and Dimethylformamide (DMF, 99%) were provided by Sigma-Aldrich Co. LLC. Formic acid (98%) was purchased from Sinopharm Chemical Reagent Co., Ltd. (Shanghai, China). All the reagents and solvents were used without further purification. The tip-type sonication machine (Bilon-1000Y) was manufactured by Shanghai Bilon Instrument Manufacturing Co., Ltd. (Shanghai, China). Ultrasonic bath SK5210LHC was from Shanghai Kudos Ultrasonic Instrument Co., Ltd. (Shanghai, China). Centrifugal machine (TGL-10C) was from Anting Scientific Instrument Factory (Shanghai, China).

2.2. Preparation of s-BN and s-GH. s-BN was prepared by exfoliation of the BN powder with a tip-type sonication process.[12] BN power (1 g) dispersed in 40 mL DMF was vigorously sonicated for 10 h to peel away BN nanoparticles and then was centrifuged at 8000 rpm

DOI: 10.1021/acsami.5b04444
ACS Appl. Mater. Interfaces 2015, 7, 19068−19075

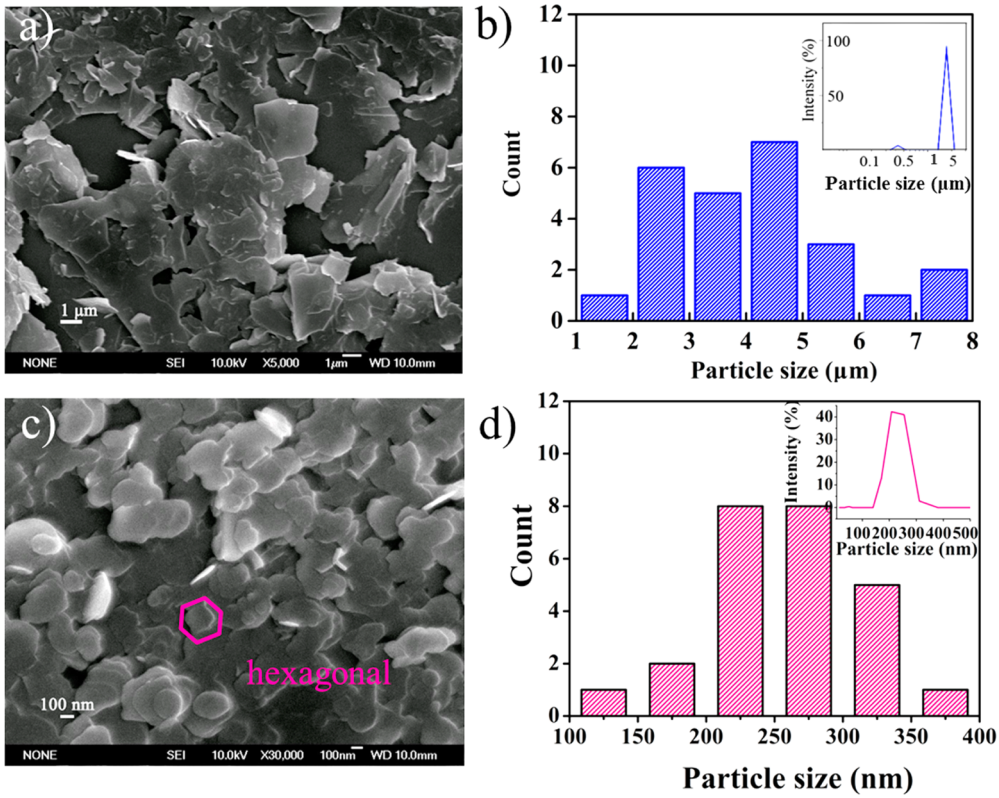

Figure 2. (a) SEM image of s-GH. (b) Statistics of s-GH size based on 25 sheets in SEM image. (c) SEM image of s-BN. (d) Statistics of s-BN size based on 25 sheets in SEM image. (Inset, b) s-GH and (inset d) s-BN size distribution measurement (Zetasizer).

for 10 min. The liquid supernatant was collected subsequently and one unit of s-BN suspension (~1.5 mg in 40 mL) was obtained. The high content of s-BN suspension was obtained by concentrating 2 and 5 units of s-BN suspension by rotary evaporation at 80 °C for 10−15 min. Finally, 50 mL (for 2 units) and 60 mL (for 5 units) s-BN suspensions were obtained and noted as 0.6 and 1.5 wt % s-BN suspension according to the weight ratio of s-BN in the PS matrix (0.5 g), respectively. GH (25/50/100 mg) were suspended in 30 mL DMF and sonicated at 53 kHz for 2 h in the ultrasonic bath. The obtained suspensions were noted as 5, 10, and 20 wt % s-GH suspension according to the weight ratio of s-GH in the PS matrix (0.5 g), respectively.

2.3. Preparation of the Polymeric Composites. All the polymeric composites were prepared by solution blending and hot-pressing method. In a typical procedure, PS solution was prepared by dissolving 0.5 g PS in 20 mL DMF solution. Then, designed amounts of s-GH and s-BN suspension were mixed in PS solution and magnetically stirred for 30 min. Coagulation was subsequently achieved by the obtained suspension being quickly poured into 1 L of deionized water. After being repeatedly washed with deionized water and dried, the coagulation was hot-pressed to obtain the heat-conducting fins. The hot-pressing temperature was 180 °C, and the pressure was 15 MPa. The obtained PS/s-GH/s-BN composites were labeled as PSG-B (for example, PSG20-B0.6, PSG20-B1.5, where the numbers indicate the weight content of the GH and BN fillers). Similarly, the PA/s-GH/s-BN (labeled as PAG-B) composites were prepared with the same process as PSG-B composites, except that PA was dissolved in formic acid and the hot-pressing temperature was up to 230 °C, according to our previous work.[13]

The controlled samples of PS/20 wt % BN/1.5 wt % s-GH composite was prepared as follows: BN power (100 mg) was suspended in 20 mL DMF and sonicated at 53 kHz for 30 min, and then mixed with 1.5 wt % s-GH suspension and PS solution. The rest of the process was the same as the preparation of PSG-B composites. The finally obtained fins noted as PSB-G (e.g., PSB20-G0.6, PSB20-G1.5) by different weight content of fillers.

2.4. Characterization. The morphology and microstructure of s-GH and s-BN were investigated by high-resolution transmission electron microscopy (HRTEM, JEM-2010F, JEOL, Japan), Raman spectra (INVIA, Renishaw PLC, UK), scanning electron microscopy (SEM, JSM-6700F, JEOL, Japan) and atomic force microscopy (AFM, Nano Scope III A, Veeco, Plainview, NY). The size of s-BN and s-GH were determined by nanoparticle size analyzer (Zetasizer 3000HS, Malvern Instruments, U.K). The morphology and microstructure of the composites were investigated by scanning electron microscopy (SEM, JSM-6700F, JEOL, Japan) and biotransmission electron microscopy (120 kV, Tecani G2 spirit Biotwin, FEI). The thermal conductivity and micromechanical properties of the composites fins were performed on a Netzsch STA409PC simultaneous thermal analyzer and Triboindenter (instrument number 2A062480, Hysitron Co., Ltd., Minneapolis, MN), respectively. Detailed test procedures of TC and micromechanical properties were given in Supporting Information. X-ray diffraction (XRD) patterns were collected with a D/MAX2200/PC X-ray diffractometer with Cu Kα radiation (λ = 0.154 nm).

3. RESULTS AND DISCUSSION

BN and GH can be exfoliated to monolayer or few-layer 2-D nanosheets via sonication with the help of DMF solvent molecules entering the lattice of the sheet.[4] The exfoliated s-BN and s-GH sheets maintained the uniform dispersion statues in DMF solution even after more than 1 month (Figure 1a). The s-BN suspension showed obvious Tyndall effect, suggesting the small particle size and uniform dispersion of s-BN sheet.[14] However, the Tyndall effect can not be observed in s-GH suspension, suggesting a larger particle size of s-GH than s-BN. Raman spectra of s-GH (Figure 1e) displayed a stronger D band at 1368 cm^{-1}, implying a larger density of edge-plane sites as the stacked layer exfoliated.[12,15] s-GH sheets exhibited folded and curled morphology by TEM analysis (Figure 1b). The

DOI: 10.1021/acsami.5b04444
ACS Appl. Mater. Interfaces 2015, 7, 19068−19075

thickness of s-GH (5.1 nm, Figure 1c) was reduced compared to the origin GH particles (6−8 nm), which indicated that GH particles were exfoliated into smaller ones by the vibration-induced exfoliation. The Raman peak of s-BN at 1365 cm^{-1} blue-shifted to 1367 cm^{-1} (Figure 1f), which was caused by a hardening of the corresponding E_{2g} phonon mode in monolayers and indicated that the s-BN sample might be exfoliated into monolayers.[16,17] Gorbachev and co-workers[18] also found the 2−4 cm^{-1} blue-shift for BN monolayer. The full width at half-maximum of Raman characteristic peak of s-BN was narrower than 30 cm^{-1}, suggesting that s-BN sheets had good (002) crystallinity.[19] TEM image (Figure 1d) showed that s-BN had a size of about 200 nm and the surface of s-BN sheets was smooth. Few-layer s-BN sheet was identified easily by its edge. As observed in the fast Fourier transform (FFT, Figure 1d inset) of the image, only intense (1100) dots were seen, indicating of a few-layer (may be monolayer) s-BN.[20] Three- to few-layer stacked s-BN sheets were also found in Figure 1d and other few-layer s-BN were showed in Figure S-1. The distance interlayer of s-BN was approximate as 0.34 nm (Figure S-1), which is in good agreement with other reports.[4,12] The thickness of s-BN was about 1.3 nm (3 layers[16]) with the AFM measurements (Figure 1g), which confirmed that few-layers s-BN was obtained. The thin thickness and high crystalline quality of s-BN fillers were propitious to improve the thermal conductive and mechanical properties of the composites.

Figure 2 shows the morphologies of s-GH and s-BN nanosheets. s-GH (Figure 2a) were irregular sheet-like, while s-BN were smooth hexagonal (Figure 2c), which is consistent with TEM images. For the particle size distribution, it is compatible of the results from statistic of SEM images and equipmental analysis (Figure 2b,d). The average size of s-GH (4.79 μm) was about 20 times bigger than that of s-BN (218.3 nm).

Figure 3 gave the TC of polystyrene (PS) composites by the transient laser flash technique (details see Supporting Information). The TC of pure PS was 0.155 $W{\cdot}m^{-1}K^{-1}$. With the increase of filler content, TC of the composites increased consistently. For example, the TC of PSG20 composites with 20 wt % s-GH loading reached 0.480 $W{\cdot}m^{-1}K^{-1}$. This is a reasonable value compared to 0.3 $W{\cdot}m^{-1}K^{-1}$ of PS/10 vol % reduced graphene oxide composite[21] and 0.5 $W{\cdot}m^{-1}K^{-1}$ of PS/20 wt % graphite composite.[22] After further compounded 1.5 wt % s-BN, the TC of PSG20-B1.5 reached up to 0.662 $W{\cdot}m^{-1}K^{-1}$, significantly enhanced by 38% relative to PSG20 and 327% to pure PS. The results showed that s-BN had a strong synergistic effect with s-GH for improving the TC of PS matrix. For example, the TC of the PS composite was 0.662 $W{\cdot}m^{-1}K^{-1}$ with 21.5 wt % filler loading in our work, which was far higher than 0.32 $W{\cdot}m^{-1}K^{-1}$ of PS with 20 wt % MWCT/C foam[23] and 0.42 $W{\cdot}m^{-1}K^{-1}$ of PS with 20 vol % AlN[24] and was comparable to 0.62 $W{\cdot}m^{-1}K^{-1}$ of the PS composite with 30 wt % single wall carbon nanotubes (SWCNTs)[25] (Table 1).

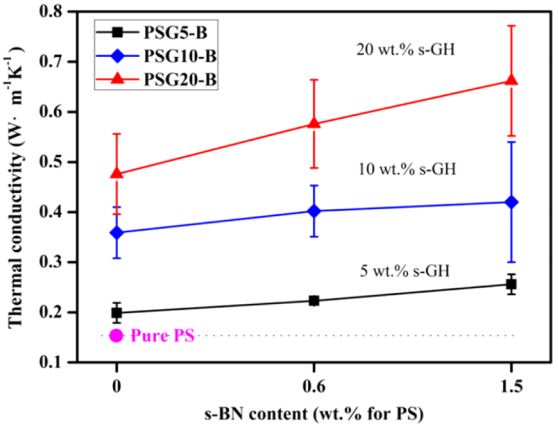

Figure 3. TC of the PS composites with varied s-BN and s-GH contents. The data are average of three samples, and the relative errors for each data point are reported as well.

Table 1. Comprehensive Comparison on the TC Enhancement of PS Composites with Inorganic Fillers

matrix	type of filler	filler content	TC ($W{\cdot}m^{-1}K^{-1}$)	ref
neat PS			0.155	
PS	reduced oxide graphene	10 vol %	0.30	21
PS	MWCNT/C foam	20 wt %	0.32	23
PS	AlN	20 vol %	0.42	24
PS	SiCp/SiCw	20 vol %	0.40	26
PS	graphite	20 vol %	0.50	22
PS	SWCNTs	30 wt %	0.62	25
PS	MWNTs-*g*-SMA	33.3 vol %	0.89	27
PS	s-GH/s-BN	21.5 wt %	0.66	this work

In the present work, we proposed a simulation schematic for the synergistic effect as shown in Figure 4d. As a low quantity of s-GH (<5 wt %) distributed in PS matrix, TC showed a slightly increase after embedded s-GH and s-BN, this was because the main thermal resistance probably originated from the polymer matrix. With s-GH up to 10 wt %, the percolating network of s-GH formed. The TC of PSG increased to 0.48 $W{\cdot}m^{-1}K^{-1}$ for PSG20. However, the enhancement of TC per 1 wt % s-GH was only 0.016 $W{\cdot}m^{-1}K^{-1}$ with 20 wt % s-GH loading (from 0.155 to 0.48 $W{\cdot}m^{-1}K^{-1}$). This may be caused by a lot of interspaces suppressing the formation of s-GH percolating network and precluding direct s-GH to s-GH phonon transfer (Figure S2).[8,28,29] The TC of PSG20-B1.5 improved from 0.48 (PSG20) to 0.662 $W{\cdot}m^{-1}K^{-1}$ with further 1.5 wt % s-BN loading and the enhancement of TC with per 1 wt % s-BN synchronously rose up to 0.12 $W{\cdot}m^{-1}K^{-1}$, which was almost 8 times higher than that of individual 20 wt % s-GH. This was because s-BN sheets could fill into the interspaces of s-GH due to its 20 fold smaller size as showed in the SEM image of PSG20-B1.5 (Figure 4b), which meant that s-BN patched up the broken thermal conductive connects. Compared to 1D filler such as CNTs cylinder, s-BN probably provided increased area of interface contact than 1D filler because the extended dimensionality and large contact area tend to decrease interfacial resistance between the fillers.[9,30] The reformed s-GH/s-BN thermal conductive networks helped to improve the thermal conductivity (Figure 4b). Moreover, the other factor for the TC enhancement in the through-plane direction would be the stacked structure formed by s-BN covering on the surface of s-GH and PS matrix, as shown in Figure 4c. The stacked structure could be regard as paralleling a low thermal resistance of s-BN within the total resistance of s-GH and PS matrix according to the paralleling thermal resistance model proved by graphene added in graphite/polymer composites.[28]

DOI: 10.1021/acsami.5b04444
ACS Appl. Mater. Interfaces 2015, 7, 19068−19075

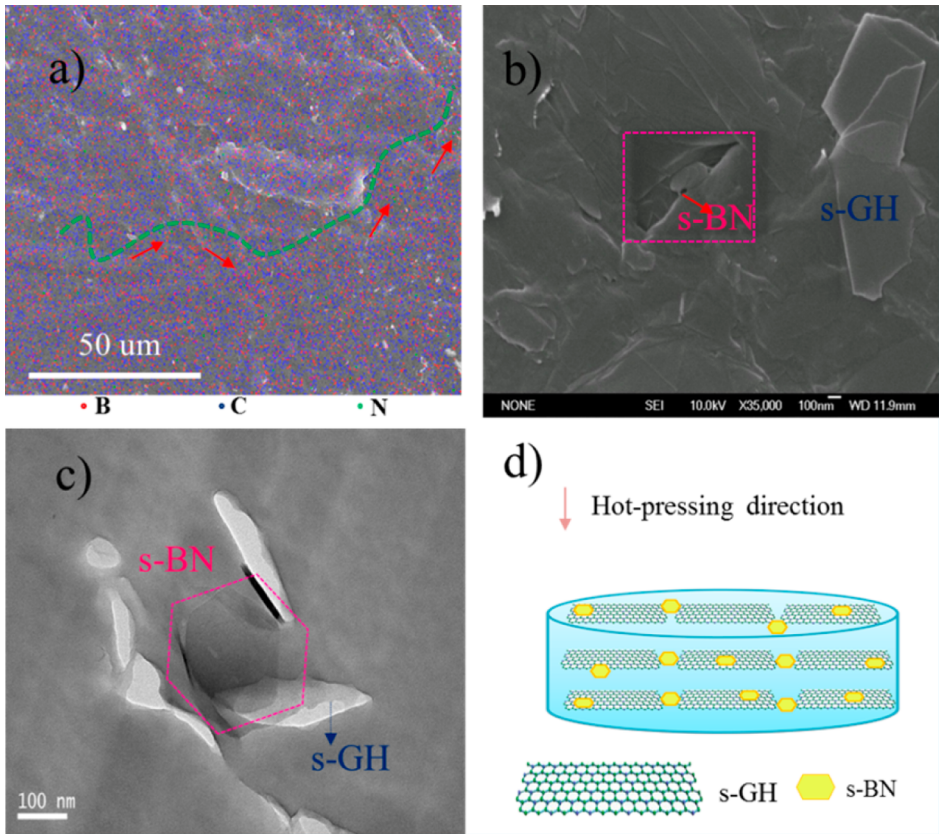

Figure 4. (a) Elemental analysis on the surface of PSG20-B1.5 composite: (red dot) B, (blue dot) C, and (green dot) N. The red raw stands for the heat flow within the s-GH/s-BN network. (b) High-resolution SEM image of the PSG20-B1.5 composite. (c) TEM image of the PSG20-B1.5 composite. (d) Simulation schematic for the inherent structure of PSG-B composites.

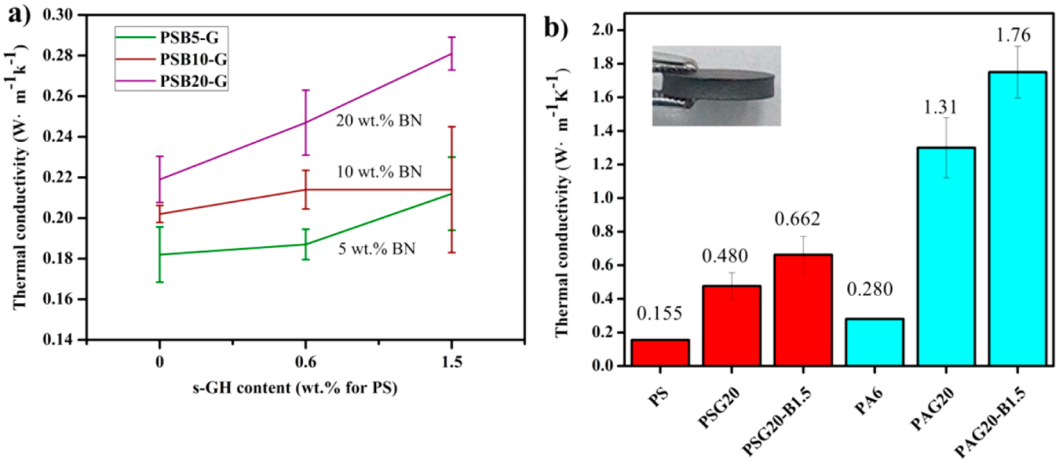

Figure 5. (a) TC of the PSB-G composites with varied BN and s-GH loading. (b) Comparison of TC between PS composites and PA composites and (inset) photograph of PSG20-B1.5 fin, about 1.5 mm thickness. The data for panels a and b are averages of three independent measurements and three samples, respectively.

The total thermal resistance was reduced as hexagonal s-BN nanosheets were inserted into s-GH sheets in the bulk material. Alternatively, we utilized 1.5 wt % s-GH (4.79 μm) filled into 20 wt % BN (1 μm) with PS matrix (Figure 5a). The TC of PSB20-G1.5 was 0.275 $W{\cdot}m^{-1}K^{-1}$, which was far less than PSG20-B1.5 (0.662 $W{\cdot}m^{-1}K^{-1}$). The reason would be large s-GH could not patch up the interspaces between smaller BN, and thus, an effective thermal conductive network within s-GH/BN filler would not form, which conversely supported our proposed schematic in Figure 4d. Another possible positive factor for the bridging of small s-BN may be the flat surface. It was put forward that the contribution of the phonon acoustic mismatch to the interface contact resistance increases with decreasing radius of the nano particles, and the flat surface and the rigidity of graphene militate in favor of increasing the TC of polymers.[30,3132] Here, the small s-BN also kept its flat surface (Figures 1d and 4b,c and Figure S-1), which might help to preserve the high aspect ratio of s-BN and minimize the geometric contribution to the thermal interface resistance at nanoparticle−nanoparticle interfaces.[30]

DOI: 10.1021/acsami.5b04444
ACS Appl. Mater. Interfaces 2015, 7, 19068−19075

We suggested that the synergistic effect of s-BN and s-GH was not for some specific polymer rather than varieties of polymers, so we applied this hybrid filler for the crystalline polyamide-6 (PA). As show in Figure 5b, TC of PAG20 increased from 1.31 to 1.76 $W{\cdot}m^{-1}K^{-1}$ (PAG20-B1.5) for further 1.5 wt % s-BN loading, which improved by 625% relative to neat PA composites. The enhancement for PA was higher than the enhancement (327%) for PS with the same filler loading, perhaps because the high order of the molecular chains in the crystalline area would help to vibrate the crystal lattice and finally increase the TC of polymers (XRD pattern, see Figure S3).[33] Table 2 shows TC as a function of filler fraction for PA materials according to published reports. It is easy to find the superiority of our method. For example, the TC of the PA composite is 1.76 $W{\cdot}m^{-1}K^{-1}$ in the present work, which is far higher than 1.08 $W{\cdot}m^{-1}K^{-1}$ of 40 wt % graphite/PA composite[34] and 1.37 $W{\cdot}m^{-1}K^{-1}$ of 30 wt % graphite/PA composite[35] (Table 2). Compared to the TC value with comparable filler loading, 1.76 $W{\cdot}m^{-1}K^{-1}$ of PAG20-B1.5 composite was also higher than 0.88 $W{\cdot}m^{-1}K^{-1}$ of epoxy with microscale h-BN (40 wt %) and nanoscale α-Al_2O_3 (10 wt %)[36] and 1.2 $W{\cdot}m^{-1}K^{-1}$ of polyimide (PI) with 21 wt % of micro and 9 wt % nano sized BN fillers.[37] Recently, Tsai et al.[10] increased the TC of PI to 2.21 $W{\cdot}m^{-1}K^{-1}$ with 50 wt % functionalized BN and 1 wt % glycidyl methacrylate-grafted graphene hybrid filler. However, we have different cogitations that we used few-layers of two 2-D fillers while they enhanced the interface coupling by functionalized fillers. Our strengths lay in a simple experimental procedure, achieving a high thermal conductivity, while they keep the PI composites flexibile. The high TC for polymer materials with relatively low filler loading in the present work have a potential industrial application in high-performance thermal management systems because low filler loading is important for decreasing the viscosity and improving the processability of thermal interface materials.[8,30]

Table 2. Comprehensive Comparison on the Improvement in Thermal Conductivities of PA Composites with Inorganic Fillers

matrix	type of filler	filler content (wt %)	TC ($W{\cdot}m^{-1}K^{-1}$)	ref
neat PA6			0.28	
PA6	reduced graphite oxide	10	0.42	13
PA66	carbon fiber	20	0.48	38
PA66	graphite	20	0.60	39
PA6	organo-montmorllonite	20	0.45	40
PA6	carbon fiber	30	0.32	33
PA6	graphite	30	1.37	35
PA66	graphite	40	1.08	34
PA6	graphite/carbon fiber	60	2.03	6
PA6	s-GH/s-BN	21.5	1.76	this work

As mentioned above, high filler loading may result in the loss of mechanical integrity of the polymer materials. However, in the present work, we found mechanical properties of the composites enhanced synchronously with TC. Figure 6a,b displayed Young's modulus (E) and microhardness (H) of the composites by nanoindentation technique which is a widely used method to the characterize the mechanical behavior of materials at small scales.[41] The results (Figure 6) showed that E and H of neat PS were 0.14 and 4.32 GPa, respectively, which were roughly consistent with the reported value 0.17 GPa[42,43] and 2−5 GPa.[44] The values significantly increased with the loading of fillers. It was obvious that from PSG20 to PSG20-B1.5, E increased from 4.7 to 6.3 GPa, and H increased from 0.2 to 0.25 GPa, improvements of 34 and 25%, respectively, with just 1.5 wt % s-BN loading. On one hand, this was because the interspaces were filled with s-BN (Figure 4b), which made the load almost forced on rigid s-GH and s-BN sheets. On the other hand, when s-BN covered on s-GH (Figure 4c), it might change the stress distribution and retrained the crack from propagating on the interfaces between fillers and polymer, which finally made the energy dispersed on the surface of s-GH and s-BN sheets.[3] Compared with previous investigations on other dimension filler polymeric composites, the improvement of mechanical properties with 1.5 wt % s-BN loading in this work were relative high. For example, the elastic modulus of poly(methyl methacrylate) (PMMA) increased from 4.02 to 4.83 GPa (20% improvement) with 20 wt % nano-SiO_2 loading.[45] The microhardness of PA increased from approximately 0.11 to 0.14 GPa (28% improvement) with 4 wt % CNTs loading.[46] In the case of PA, E and H of PAG20-B1.5 (4.8 and 0.18 GPa, respectively) also increased compared to PAG20 (4.5 and 0.17 GPa, respectively). Comparing to the enhancement in TC, the enhancement in mechanical properties for PA was not significant. The possible reason may relate to

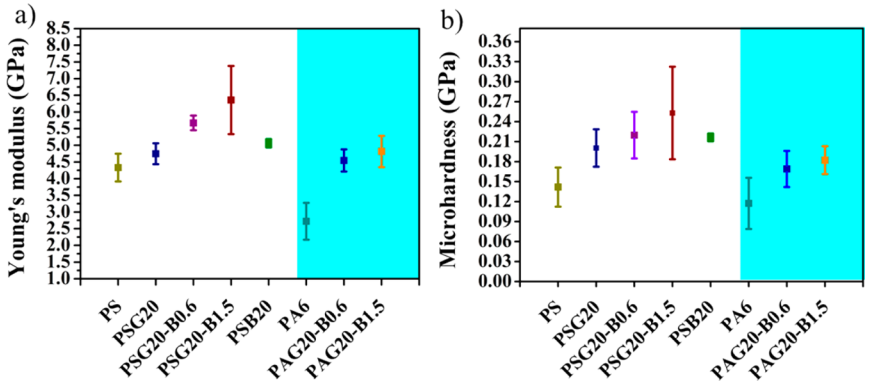

Figure 6. Mechanical properties of the PSG-B and PAG-B composites by nanoindentation technique (a) microhardness (H) and (b) Young's modulus (E). All the samples were derived from at least five indentations. Test conditions: 10 mN, 5 × 5 × 5 s.

DOI: 10.1021/acsami.5b04444
ACS Appl. Mater. Interfaces 2015, 7, 19068−19075

the decreasing of crystallinity caused by the incorporation of the filler[46] and the details are deferred for later study.

4. CONCLUSION

In the present work, we achieved a synergistic effect of nano sized s-BN with micro sized s-GH in the enhancement of TC and mechanical properties for polymeric composites. An additional introduction of 1.5 wt % s-BN could increase the TC up to 38 and 34% in polystyrene (PS) and polyamide (PA), respectively, comparing with the composites containing 20 wt % s-GH. Meanwhile, the mechanical properties of the composites were enhanced with the small amount BN loading. The synergism originated from three aspects: (1) s-BN filled into the interspaces of s-GH, which led to extended contact along the filler thermal networks; (2) the stacked structure of s-BN/s-GH formed, which was conducive for decreasing thermal resistance and stress dispersion; and (3) the flat surface of small s-BN helps preserve its high aspect ratio and minimize the geometric contribution to the thermal interface resistance at nanoparticle−nanoparticle interfaces. The obtained polymeric materials have potential applications in thermal interface materials, connectors, and other high performance thermal management systems.

■ ASSOCIATED CONTENT

Supporting Information

The Supporting Information is available free of charge on the ACS Publications website at DOI: 10.1021/acsami.5b04444.

TEM images of s-BN and s-GH, SEM images on different area of the PSG-B surface, XRD patterns, and detailed test procedure of TC. (PDF)

■ AUTHOR INFORMATION

Corresponding Authors

*E-mail: dingpeng@shu.edu.cn.
*E-mail: shiliyi@shu.edu.cn.

Notes

The authors declare no competing financial interest.

■ ACKNOWLEDGMENTS

Dr. P. Ding acknowledges the financially support from the National Natural Science Foundation of China (51303101). The authors thank Prof. Yuliang Chu and Prof. Weijun Yu for help with the SEM and TEM measurements.

■ REFERENCES

(1) Stankovich, S.; Dikin, D. A.; Dommett, G. H. B.; Kohlhaas, K. M.; Zimney, E. J.; Stach, E. A.; Piner, R. D.; Nguyen, S. T.; Ruoff, R. S. Graphene-Based Composite Materials. *Nature* **2006**, *442*, 282−286.

(2) Taha-Tijerina, J.; Narayanan, T. N.; Gao, G. H.; Rohde, M.; Tsentalovich, D. A.; Pasquali, M.; Ajayan, P. M. Electrically Insulating Thermal Nano-Oils Using 2d Fillers. *ACS Nano* **2012**, *6*, 1214−1220.

(3) Vinod, S.; Tiwary, C. S.; da Silva Autreto, P. A.; Taha-Tijerina, J.; Ozden, S.; Chipara, A. C.; Vajtai, R.; Galvao, D. S.; Narayanan, T. N.; Ajayan, P. M. Low-Density Three-Dimensional Foam Using Self-Reinforced Hybrid Two-Dimensional Atomic Layers. *Nat. Commun.* **2014**, *5*, 4541.

(4) Coleman, J. N.; Lotya, M.; O'Neill, A.; Bergin, S. D.; King, P. J.; Khan, U.; Young, K.; Gaucher, A.; De, S.; Smith, R. J.; Shvets, I. V.; Arora, S. K.; Stanton, G.; Kim, H. Y.; Lee, K.; Kim, G. T.; Duesberg, G. S.; Hallam, T.; Boland, J. J.; Wang, J. J.; Donegan, J. F.; Grunlan, J. C.; Moriarty, G.; Shmeliov, A.; Nicholls, R. J.; Perkins, J. M.; Grieveson, E. M.; Theuwissen, K.; McComb, D. W.; Nellist, P. D.; Nicolosi, V. Two-Dimensional Nanosheets Produced by Liquid Exfoliation of Layered Materials. *Science* **2011**, *331*, 568−571.

(5) Tang, Z. H.; Kang, H. L.; Shen, Z. L.; Guo, B. C.; Zhang, L. Q.; Jia, D. M. Grafting of Polyester onto Graphene for Electrically and Thermally Conductive Composites. *Macromolecules* **2012**, *45*, 3444−3451.

(6) Yoo, Y.; Lee, H. L.; Ha, S. M.; Jeon, B. K.; Won, J. C.; Lee, S. G. Effect of Graphite and Carbon Fiber Contents on Themorphology and Properties of Thermally Conductive Composites Based on Polyamide 6. *Polym. Int.* **2014**, *63*, 151−157.

(7) Uetani, K.; Ata, S.; Tomonoh, S.; Yamada, T.; Yumura, M.; Hata, K. Elastomeric Thermal Interface Materials with High through-Plane Thermal Conductivity from Carbon Fiber Fillers Vertically Aligned by Electrostatic Flocking. *Adv. Mater.* **2014**, *26*, 5857−5862.

(8) Yu, A. P.; Ramesh, P.; Sun, X. B.; Bekyarova, E.; Itkis, M. E.; Haddon, R. C. Enhanced Thermal Conductivity in a Hybrid Graphite Nanoplatelet - Carbon Nanotube Filler for Epoxy Composites. *Adv. Mater.* **2008**, *20*, 4740−4741.

(9) Yang, S. Y.; Lin, W. N.; Huang, Y. L.; Tien, H. W.; Wang, J. Y.; Ma, C. C. M.; Li, S. M.; Wang, Y. S. Synergetic Effects of Graphene Platelets and Carbon Nanotubes on the Mechanical and Thermal Properties of Epoxy Composites. *Carbon* **2011**, *49*, 793−803.

(10) Tsai, M. H.; Tseng, I. H.; Chiang, J. C.; Li, J. J. Flexible Polyimide Films Hybrid with Functionalized Boron Nitride and Graphene Oxide Simultaneously to Improve Thermal Conduction and Dimensional Stability. *ACS Appl. Mater. Interfaces* **2014**, *6*, 8639−8645.

(11) Liem, H.; Choy, H. S. Superior Thermal Conductivity of Polymer Nanocomposites by Using Graphene and Boron Nitride as Fillers. *Solid State Commun.* **2013**, *163*, 41−45.

(12) Zhi, C. Y.; Bando, Y.; Tang, C. C.; Kuwahara, H.; Golberg, D. Large-Scale Fabrication of Boron Nitride Nanosheets and Their Utilization in Polymeric Composites with Improved Thermal and Mechanical Properties. *Adv. Mater.* **2009**, *21*, 2889−2890.

(13) Ding, P.; Su, S. S.; Song, N.; Tang, S. F.; Liu, Y. M.; Shi, L. Y. Highly Thermal Conductive Composites with Polyamide-6 Covalently-Grafted Graphene by an in Situ Polymerization and Thermal Reduction Process. *Carbon* **2014**, *66*, 576−584.

(14) Matijevic, E. Preparation and Properties of Uniform Size Colloids. *Chem. Mater.* **1993**, *5*, 412−426.

(15) Graf, D.; Molitor, F.; Ensslin, K.; Stampfer, C.; Jungen, A.; Hierold, C.; Wirtz, L. Spatially Resolved Raman Spectroscopy of Single- and Few-Layer Graphene. *Nano Lett.* **2007**, *7*, 238−242.

(16) Li, L. H.; Cervenka, J.; Watanabe, K.; Taniguchi, T.; Chen, Y. Strong Oxidation Resistance of Atomically Thin Boron Nitride Nanosheets. *ACS Nano* **2014**, *8*, 1457−1462.

(17) Li, L. H.; Santos, E. J. G.; Xing, T.; Cappelluti, E.; Roldan, R.; Chen, Y.; Watanabe, K.; Taniguchi, T. Dielectric Screening in Atomically Thin Boron Nitride Nanosheets. *Nano Lett.* **2015**, *15*, 218−223.

(18) Gorbachev, R. V.; Riaz, I.; Nair, R. R.; Jalil, R.; Britnell, L.; Belle, B. D.; Hill, E. W.; Novoselov, K. S.; Watanabe, K.; Taniguchi, T.; Geim, A. K.; Blake, P. Hunting for Monolayer Boron Nitride: Optical and Raman Signatures. *Small* **2011**, *7*, 465−468.

(19) Liu, F.; Mo, X. S.; Gan, H. B.; Guo, T. Y.; Wang, X. B.; Chen, B.; Chen, J.; Deng, S. Z.; Xu, N. S.; Sekiguchi, T.; Golberg, D.; Bando, Y. Cheap, Gram-Scale Fabrication of BN Nanosheets Via Substitution Reaction of Graphite Powders and Their Use for Mechanical Reinforcement of Polymers. *Sci. Rep.* **2014**, *4*, 4211.

(20) Sun, Z. Y.; Poller, S.; Huang, X.; Guschin, D.; Taetz, C.; Ebbinghaus, P.; Masa, J.; Erbe, A.; Kilzer, A.; Schuhmann, W.; Muhler, M. High-Yield Exfoliation of Graphite in Acrylate Polymers: A Stable Few-Layer Graphene Nanofluid with Enhanced Thermal Conductivity. *Carbon* **2013**, *64*, 288−294.

(21) Park, W.; Hu, J. N.; Jauregui, L. A.; Ruan, X. L.; Chen, Y. P. Electrical and Thermal Conductivities of Reduced Graphene Oxide/Polystyrene Composites. *Appl. Phys. Lett.* **2014**, *104*, 113101.

(22) Tu, H. M.; Ye, L. Thermal Conductive PS/Graphite Composites. *Polym. Adv. Technol.* **2009**, *20*, 21−27.

DOI: 10.1021/acsami.5b04444
ACS Appl. Mater. Interfaces 2015, 7, 19068−19075

(23) Ji, L. J.; Stevens, M. M.; Zhu, Y. F.; Gong, Q. M.; Wu, J. J.; Liang, J. Preparation and Properties of Multi-Walled Carbon Nanotube/Carbon/Polystyrene Composites. *Carbon* **2009**, *47*, 2733−2741.
(24) Yu, S. Z.; Hing, P.; Hu, X. Thermal Conductivity of Polystyrene-Aluminum Nitride Composite. *Composites, Part A* **2002**, *33*, 289−292.
(25) Peters, J. E.; Papavassiliou, D. V.; Grady, B. P. Unique Thermal Conductivity Behavior of Single-Walled Carbon Nanotube-Polystyrene Composites. *Macromolecules* **2008**, *41*, 7274−7277.
(26) Gu, J. W.; Zhang, Q. Y.; Dang, J.; Yin, C. J.; Chen, S. J. Preparation and Properties of Polystyrene/SiCw/SiCp Thermal Conductivity Composites. *J. Appl. Polym. Sci.* **2012**, *124*, 132−137.
(27) Tu, H. M.; Ye, L. Preparation and Characterization of Thermally Conductive Polystyrene/Carbon Nanotubes Composites. *J. Appl. Polym. Sci.* **2010**, *116*, 2336−2342.
(28) Zhou, S. X.; Chiang, S. W.; Xu, J. Z.; Du, H. D.; Li, B. H.; Xu, C. J.; Kang, F. Y. Modeling the in-Plane Thermal Conductivity of a Graphite/Polymer Composite Sheet with a Very High Content of Natural Flake Graphite. *Carbon* **2012**, *50*, 5052−5061.
(29) Zhou, S. X.; Xu, J. Z.; Yang, Q. H.; Chiang, S. W.; Li, B. H.; Du, H. D.; Xu, C. J.; Kang, F. Y. Experiments and Modeling of Thermal Conductivity of Flake Graphite/Polymer Composites Affected by Adding Carbon-Based Nano-Fillers. *Carbon* **2013**, *57*, 452−459.
(30) Yu, A. P.; Ramesh, P.; Itkis, M. E.; Bekyarova, E.; Haddon, R. C. Graphite Nanoplatelet-Epoxy Composite Thermal Interface Materials. *J. Phys. Chem. C* **2007**, *111*, 7565−7569.
(31) Prasher, R. S.; Chang, J. Y.; Sauciuc, I.; Narasimhan, S.; Chau, D.; Chrysler, G.; Myers, A.; Prstic, S.; Hu, C. Nano and Micro Technology-Based Next-Generation Package-Level Cooling Solutions. *Intel. Technol. J.* **2005**, *09*, 285−292.
(32) Warzoha, R. J.; Fleischer, A. S. Effect of Graphene Layer Thickness and Mechanical Compliance on Interfacial Heat Flow and Thermal Conduction in Solid-Liquid Phase Change Materials. *ACS Appl. Mater. Interfaces* **2014**, *6*, 12868−12876.
(33) Yan, X. L.; Imai, Y.; Shimamoto, D.; Hotta, Y. Relationship Study between Crystal Structure and Thermal/Mechanical Properties of Polyamide 6 Reinforced and Unreinforced by Carbon Fiber from Macro and Local View. *Polymer* **2014**, *55*, 6186−6194.
(34) Weber, E. H.; Clingerman, M. L.; King, J. A. Thermally Conductive Nylon 6,6 and Polycarbonate Based Resins. I. Synergistic Effects of Carbon Fillers. *J. Appl. Polym. Sci.* **2003**, *88*, 112−122.
(35) Zhou, S. T.; Chen, Y.; Zou, H. W.; Liang, M. Thermally Conductive Composites Obtained by Flake Graphite Filling Immiscible Polyamide 6/Polycarbonate Blends. *Thermochim. Acta* **2013**, *566*, 84−91.
(36) Fang, L. J.; Wu, C.; Qian, R.; Xie, L. Y.; Yang, K.; Jiang, P. K. Nano-Micro Structure of Functionalized Boron Nitride and Aluminum Oxide for Epoxy Composites with Enhanced Thermal Conductivity and Breakdown Strength. *RSC Adv.* **2014**, *4*, 21010−21017.
(37) Li, T. L.; Hsu, S. L. C. Enhanced Thermal Conductivity of Polyimide Films Via a Hybrid of Micro- and Nano-Sized Boron Nitride. *J. Phys. Chem. B* **2010**, *114*, 6825−6829.
(38) Heiser, J. A.; King, J. A. Thermally Conductive Carbon Filled Nylon 6,6. *Polym. Compos.* **2004**, *25*, 186−193.
(39) Miller, M. G.; Keith, J. M.; King, J. A.; Hauser, R. A.; Moran, A. M. Comparison of the Guarded-Heat-Flow and Transient-Plane-Source Methods for Carbon-Filled Nylon 6,6 Composites: Experiments and Modeling. *J. Appl. Polym. Sci.* **2006**, *99*, 2144−2151.
(40) Zhou, H.; Zhang, S. M.; Yang, M. S. The Thermal Conductivity of Nylon 6/Clay Nanocomposites. *J. Appl. Polym. Sci.* **2008**, *108*, 3822−3827.
(41) Oliver, W. C.; Pharr, G. M. An Improved Technique for Determining Hardness and Elastic Modulus Using Load and Displacement Sensing Indentation Experiments. *J. Mater. Res.* **1992**, *7*, 1564−1583.
(42) Mina, M. F.; Haque, M. E.; Balta Calleja, F. J.; Asano, T.; Alam, M. M. Microhardness Studies of the Interphase Boundary in Rubber-Softened Glassy Polymer Blends Prepared with/without Compatibilizer. *J. Macromol. Sci., Part B: Phys.* **2004**, *B43*, 1005−1014.
(43) Balta-Calleja, F. J.; Cagiao, M. E.; Adhikari, R.; Michler, G. H. Relating Microhardness to Morphology in Styrene/Butadiene Block Copolymer/Polystyrene Blends. *Polymer* **2004**, *45*, 247−254.
(44) Chizhik, S. A.; Huang, Z.; Gorbunov, V. V.; Myshkin, N. K.; Tsukruk, V. V. Micromechanical Properties of Elastic Polymeric Materials as Probed by Scanning Force Microscopy. *Langmuir* **1998**, *14*, 2606−2609.
(45) Lach, R.; Kim, G. M.; Michler, G. H.; Grellmann, W.; Albrecht, K. Indentation Fracture Mechanics for Toughness Assessment of PMMA/SiO_2 Nanocomposites. *Macromol. Mater. Eng.* **2006**, *291*, 263−271.
(46) Adhikari, R.; Khatri, S. K.; Adhikari, S.; Michler, G. H.; Calleja, F. J. B. Microindentation Hardness of Nanostructured Thermoplastic Materials. *Macromol. Symp.* **2010**, *290*, 166−174.

DOI: 10.1021/acsami.5b04444
ACS Appl. Mater. Interfaces 2015, 7, 19068−19075